Dynamics of multimode Fabry-Perot lasers: A nonlinear analysis

Ba An Nguyen* and Paul Mandel
Optique Nonlinéaire Théorique, Université Libre de Bruxelles, Campus Plaine code postal 231, B-1050 Bruxelles, Belgium
(Received 30 July 1997)

We apply the multiple time scale method to perform a nonlinear analysis of the Tang, Statz, and deMars rate equations, which describe an N-mode Fabry-Perot laser in which all modes have an equal gain and a large loss rate. In addition to the two relaxation oscillation frequencies Ω_L and Ω_R known from the linearized analysis, we find the four frequencies $2\Omega_L$, $\Omega_R \pm \Omega_L$, and $2\Omega_R$. The signature of antiphased dynamics for the new frequencies is that there are no relaxation oscillations in the total intensity at $\Omega_R \pm \Omega_L$. The laser steady state is shown to be stable, being characterized by damping rates derived explicitly. Relations among these damping rates are obtained. We also study the role played by the initial condition in governing the manifestation of the antiphase dynamics and the relative magnitude of the modal intensity power spectrum peak heights at the two main frequencies Ω_L and Ω_R. Finally, we deal with the resonant case $\Omega_R = 2\Omega_L$. In this case, inphased dynamics is shown to appear at $2\Omega_R$, instead of at Ω_R. [S1063-651X(97)11712-3]

PACS number(s): 05.45.+b, 42.65.Sf, 42.55.Rz, 42.60.Rn

I. INTRODUCTION

The Tang, Statz, and deMars (TSD) equations [1] have recently been revisited in connection with antiphase dynamics (AD) observed in solid-state multimode free-running Fabry-Perot lasers. In these lasers, the modes of the field are standing waves and the population inversion gratings created by each mode are also standing waves. The gratings are phase insensitive because the cross-gratings play no role in the slow response of the population inversion due to their rapid oscillations at the intermode beat frequency. Thus, for this class of N-mode lasers, only $2N+1$ equations are needed for $2N+1$ real dynamical variables: N modal intensities, N population inversion gratings, and one spatially averaged population inversion. The TSD equations are those $2N+1$ equations. The most pronounced collective self-organized behavior of a multimode laser is its intensity coherence. The modal intensities may respond to perturbations at M frequencies ($M \leqslant N$), but their sum is almost or exactly vanishing at all frequencies but the highest one. This phenomenon, the so-called antiphase dynamics [2], was observed experimentally for the first time in optics [3] in a neodymium-doped yttrium aluminum garnet (Nd:YAG) laser containing a potassium titanyl phosphate (KTP) crystal responsible for the laser intracavity second-harmonic generation. Unexpectedly, however, there is an asymptotic link [4] between the rate equations modeling intracavity second-harmonic generation in a Nd:YAG laser and the TSD equations modeling a multimode Fabry-Perot laser. Both sets of equations display the same ''nonlinear nucleus,'' which is responsible for AD. It is worth noting that AD arises in a variety of circumstances: in the transient relaxation to steady state [5–7], in the presence of an external periodic modulation [8–11], in the noise spectrum of a cw laser [12], and in the chaotic regime [9,10,13–15].

From a theoretical point of view, several types of AD have been identified [16]. Antiphased solutions of specific forms have also been investigated in the context of Josephson-junction arrays [17,18] and coupled laser arrays [19,20], as well as in a more general context of coupled nonlinear oscillators [21–23]. For a solid-state Fabry-Perot laser operating on N modes, the signature of AD is as follows. The modal intensities have a response to an external perturbation which is characterized, in general, by N frequencies $\Omega_1 > \Omega_2 > \cdots > \Omega_N$ such that the oscillations are always in-phased at Ω_1 and perfectly or partially antiphased at all other frequencies. This has been derived analytically and confirmed experimentally for $N=2$ in [24] and $N=3$ in [25–27]. In [27,28] different types of self-organization associated with AD have been conjectured for any number N of lasing modes as well. The simplest model, solvable for an arbitrary mode number N, is the reference model [29], in which all the modes are assumed to have the same gain and an infinite loss rate. The effect of an arbitrary loss rate has recently been taken into account in [30] and in a generalized reference model [31]. A somewhat different approach has been followed in [32]. In both reference models [29] and [31], AD has explicitly been shown to be a universal property in the dynamics of multimode Fabry-Perot lasers, i.e., it is free from the system preparation.

Most analytical results available up to now have been obtained from the linearized theory. A notable exception is a global stability theorem that proves that the steady-state solution of the rate equations is stable if the population inversion is everywhere positive [33,34]. Although the linearization approximation succeeds in capturing the essential aspects of the laser dynamics, it is still far from a complete description of the problem. The purpose of this paper is to progress beyond the linearized theory to get better insight into AD. We consider a model that is somewhat intermediate between those of [29] and [31]. Namely, we assume an equal gain and a finite but large loss rate for all modes. Introducing multiple time scales suggested by the linearized stability analysis, we perform a nonlinear analysis of the TSD equations. As a result, we find a distinctive signature of AD, derive explicit expressions for the damping rates, clarify the

*Permanent address: The Institute of Physics, P.O. Box 429, Bo Ho, Hanoi, Vietnam.

initial-condition-dependent manifestation of AD, and establish relationships between the modal intensity power spectra peak heights at different relaxation oscillation frequencies. In parallel with the theoretical treatment, we also carry out numerical simulations using the full TSD equations. We obtain good agreement between the analytical and numerical results.

Our paper is organized as follows. After the Introduction, we construct in Sec. II the nonlinear evolution equations for the deviation from the steady state. In Sec. III we solve the nonlinear equations using the multiple time scale method, which leads to the formulation of solvability conditions. Physical aspects based on the mathematical results of Sec. III are discussed in Sec. IV. Section V deals with the resonant case to which the analysis done in Sec. III is not applicable. Concluding remarks are given in Sec. VI.

II. EVOLUTION EQUATIONS

We consider an N mode Fabry-Perot laser which can be described by the $2N+1$ TSD rate equations [1,2]

$$\varepsilon^2\frac{dI_p}{dt}=\left[\left(D-\frac{Q_p}{2}\right)\gamma_p-1\right]I_p,$$

$$\frac{dQ_p}{dt}=D\gamma_pI_p-\left(1+\sum_{q=1}^{N}\gamma_qI_q\right)Q_p, \tag{1}$$

$$\frac{dD}{dt}=w-D-\sum_{q=1}^{N}\left(D-\frac{Q_q}{2}\right)\gamma_qI_q,$$

where I_p and Q_p denote the modal intensity and population inversion grating associated with the same cavity mode at optical frequency, and D is the spatially averaged population inversion. $\gamma_p\leqslant 1$ is the modal gain in units of that of the first mode, $w\geqslant 1$ is the pump rate in units of the first mode threshold pump, and $\varepsilon=1/\sqrt{k}$ with k the modal loss rate, which is assumed to be mode-independent and scaled to the population inversion decay rate. Our interest is in lasers such as Nd:YAG or $LiNdP_4O_{12}$ lasers which have k greater than or equal to 10^4. For such lasers ε is a useful small parameter. Let

$$\mathcal{I}_p=I_p-I_p^s,\quad \varepsilon\mathcal{Q}_p=Q_p-Q_p^s,\quad \varepsilon\mathcal{D}=D-D^s$$

be the deviations from the steady state $\{I_p^s,Q_p^s,D^s\}$ of (1). The TSD equations yield for the deviations

$$\varepsilon\frac{d\mathcal{I}_p}{dt}=\gamma_p\left(\mathcal{D}-\frac{\mathcal{Q}_p}{2}\right)(I_p^s+\mathcal{I}_p),$$

$$\varepsilon\frac{d\mathcal{Q}_p}{dt}=D^s\gamma_p\mathcal{I}_p-Q_p^s\sum_{q=1}^{N}\gamma_q\mathcal{I}_q+\varepsilon\left\{\gamma_p\mathcal{D}(I_p^s+\mathcal{I}_p)-\left[1+\sum_{q=1}^{N}\gamma_q(I_q^s+\mathcal{I}_q)\right]\mathcal{Q}_p\right\}, \tag{2}$$

$$\varepsilon\frac{d\mathcal{D}}{dt}=-\sum_{q=1}^{N}\mathcal{I}_q-\varepsilon\left[\mathcal{D}+\sum_q\gamma_q\left(\mathcal{D}-\frac{\mathcal{Q}_q}{2}\right)(I_q^s+\mathcal{I}_q)\right].$$

Equations (2) are still exact. Expanding γ_p and the dynamical variables in powers of ε leads to a sequence of linear problems that may be solved sequentially. This is done in the next section.

III. MULTIPLE TIME SCALES

We seek perturbative solutions of Eqs. (2) in the form of a series in ε,

$$\mathcal{I}_p=\varepsilon(\mathcal{I}_{p0}+\varepsilon\mathcal{I}_{p1}+\cdots),\quad \mathcal{Q}_p=\varepsilon(\mathcal{Q}_{p0}+\varepsilon\mathcal{Q}_{p1}+\cdots),$$

$$\mathcal{D}=\varepsilon(\mathcal{D}_0+\varepsilon\mathcal{D}_1+\cdots), \tag{3}$$

where $\mathcal{I}_{pj}$, $\mathcal{Q}_{pj}$, and $\mathcal{D}_j$ are $\mathcal{O}(1)$. In addition, we introduce the simplifying assumption $\gamma_p=1\ \forall p$. Inserting Eq. (3) and $\gamma_p=1$ into Eq. (2) generates on both sides infinite series in powers of ε. If we truncate each side after its leading order in ε, we see that t/ε is the relevant time scale. Yet, t becomes the relevant time scale at the next order in ε, and so on. In other words, the dynamics is governed by time scales separated by powers of ε. This is confirmed by a direct linear stability analysis [2,30]. Guided by this argument, we introduce new independent multiple time scales $T_{-1},T_0,T_1,T_2,\ldots$ as

$$T_{-1}=\varepsilon^{-1}t,\quad T_0=\varepsilon^0t,\quad T_1=\varepsilon^1t,\quad T_2=\varepsilon^2t,\ldots. \tag{4}$$

Substituting Eq. (3) into Eq. (2) with the aid of the chain rule

$$\frac{d}{dt}=\frac{\partial}{\partial T_{-1}}\frac{dT_{-1}}{dt}+\frac{\partial}{\partial T_0}\frac{dT_0}{dt}+\frac{\partial}{\partial T_1}\frac{dT_1}{dt}+\cdots$$

$$=\frac{1}{\varepsilon}\frac{\partial}{\partial T_{-1}}+\frac{\partial}{\partial T_0}+\varepsilon\frac{\partial}{\partial T_1}+\cdots,$$

and equating to zero coefficients of like orders of ε, we arrive at the following sequence of equation systems.

At $\mathcal{O}(1)$

$$\frac{\partial\mathcal{I}_{p0}}{\partial T_{-1}}=\left(\mathcal{D}_0-\frac{\mathcal{Q}_{p0}}{2}\right)I,$$

$$\frac{\partial\mathcal{Q}_{p0}}{\partial T_{-1}}=d\mathcal{I}_{p0}-Q\sum_{q=1}^{N}\mathcal{I}_{q0}, \tag{5}$$

$$\frac{\partial\mathcal{D}_0}{\partial T_{-1}}=-\sum_{q=1}^{N}\mathcal{I}_{q0}.$$

At $\mathcal{O}(\varepsilon)$

$$\frac{\partial\mathcal{I}_{p1}}{\partial T_{-1}}=\left(\mathcal{D}_1-\frac{\mathcal{Q}_{p1}}{2}\right)I+\left[\frac{\mathcal{I}_{p0}}{I}\frac{\partial}{\partial T_{-1}}-\frac{\partial}{\partial T_0}\right]\mathcal{I}_{p0},$$

$$\frac{\partial\mathcal{Q}_{p1}}{\partial T_{-1}}=d\mathcal{I}_{p1}-Q\sum_{q=1}^{N}\mathcal{I}_{q1}+I\mathcal{D}_0-\left(\frac{\partial}{\partial T_0}+U\right)\mathcal{Q}_{p0}, \tag{6}$$

$$\frac{\partial\mathcal{D}_1}{\partial T_{-1}}=-\sum_{q=1}^{N}\mathcal{I}_{q1}+\left(\frac{\partial^2}{\partial T_{-1}^2}-\frac{\partial}{\partial T_0}-1\right)\mathcal{D}_0.$$

At $\mathcal{O}(\varepsilon^2)$

$$\frac{\partial \mathcal{I}_{p2}}{\partial T_{-1}} = \left(\mathcal{D}_2 - \frac{\mathcal{Q}_{p2}}{2}\right) I + \frac{1}{I}\frac{\partial}{\partial T_{-1}}\left(\mathcal{I}_{p0}\mathcal{I}_{p1} - \frac{\mathcal{I}_{p0}^3}{3I}\right) + \frac{\partial}{\partial T_0}\left(\frac{\mathcal{I}_{p0}^2}{2I} - \mathcal{I}_{p1}\right) - \frac{\partial \mathcal{I}_{p0}}{\partial T_1},$$

$$\frac{\partial \mathcal{Q}_{p2}}{\partial T_{-1}} = d\mathcal{I}_{p2} - Q\sum_{q=1}^{N} \mathcal{I}_{q2} + \left(\mathcal{I}_{p0} + \mathcal{Q}_{p0}\frac{\partial}{\partial T_{-1}}\right)\mathcal{D}_0 + I\mathcal{D}_1 - \left(\frac{\partial}{\partial T_0} + U\right)\mathcal{Q}_{p1} - \frac{\partial \mathcal{Q}_{p0}}{\partial T_1}, \tag{7}$$

$$\frac{\partial \mathcal{D}_2}{\partial T_{-1}} = -\sum_{q=1}^{N} \mathcal{I}_{q2} + \left(\frac{\partial^2}{\partial T_{-1}^2} - \frac{\partial}{\partial T_0} - 1\right)\mathcal{D}_1 + \left(\frac{2\partial}{\partial T_{-1}}\frac{\partial}{\partial T_0} - \frac{\partial^3}{\partial T_{-1}^3} + \frac{\partial}{\partial T_{-1}} - \frac{\partial}{\partial T_1}\right)\mathcal{D}_0.$$

And so on. The assumption $\gamma_p = 1 \ \forall p$ implies $I = I_p^s$, $Q = Q_p^s$, $d = D^s$ and $U = 1 + \Sigma_{q=1}^{N} I_q^s = 1 + NI$. Note that in Eqs. (5)–(7) each of the dynamical variables still depends on all the time scales $T_{-1}, T_0, T_1, \ldots$.

Let us rewrite the above systems of equations in matrix forms:

$$\frac{\partial \mathcal{Z}_0}{\partial T_{-1}} = L\mathcal{Z}_0, \tag{8}$$

$$\frac{\partial \mathcal{Z}_1}{\partial T_{-1}} = L\mathcal{Z}_1 + M_1, \tag{9}$$

$$\frac{\partial \mathcal{Z}_2}{\partial T_{-1}} = L\mathcal{Z}_2 + M_2, \tag{10}$$

where $\mathcal{Z}_j$ is a $2N+1$ column vector $\mathcal{Z}_j = \mathrm{col}(\mathcal{D}_j, \mathcal{I}_{Tj}, \mathcal{Q}_{Tj}, \mathcal{I}_{2j}, \mathcal{Q}_{2j}, \mathcal{I}_{3j}, \mathcal{Q}_{3j}, \ldots, \mathcal{I}_{Nj}, \mathcal{Q}_{Nj})$ with $\mathcal{I}_{Tj} = \Sigma_{q=1}^{N} \mathcal{I}_{qj}$ and $\mathcal{Q}_{Tj} = \Sigma_{q=1}^{N} \mathcal{Q}_{qj}$, L is a $(2N+1)\times(2N+1)$ constant matrix, and M_j are $2N+1$ column vectors that depend nonlinearly on the $\{\mathcal{Z}_k\}$ with $k<j$. In this representation L has a convenient form, given in Appendix A together with M_1 and M_2.

A. The $\mathcal{O}(1)$ problem

The $\mathcal{O}(1)$ problem consists of the homogeneous equation (8), which can be obtained directly by linearizing the right-hand side (rhs) of Eq. (2) and has been studied in [2,29] using another representation for the eigenvector. It has five distinct eigenvalues,

$$\lambda_1 = 0, \tag{11}$$

$$\lambda_j = -i\omega_L \quad \text{with} \quad j = 2,3,\ldots,N \quad \text{and} \quad \omega_L = \sqrt{Id/2}, \tag{12}$$

$$\lambda_{N+j} = +i\omega_L \quad \text{with} \quad j = 2,3,\ldots,N, \tag{13}$$

$$\lambda_{N+1} = -i\omega_R \quad \text{with} \quad \omega_R = \sqrt{I(2N+d-NQ)/2} = \sqrt{w-1}, \tag{14}$$

$$\lambda_{2N+1} = +i\omega_R. \tag{15}$$

The eigenvector associated with the zero eigenvalue is

$$\mathcal{Z}_0^{(1)} = \mathrm{col}(1/2,0,N,0,1,0,1,\ldots,0,1). \tag{16}$$

From (12) and (13) it is clear that each of the two eigenvalues $\pm i\omega_L$ is $N-1$ degenerate. The $N-1$ orthogonal eigenvectors associated with $-i\omega_L$ are

$$\mathcal{Z}_0^{(2)} = \mathrm{col}(0,0,0,-i\omega_L/d,1,0,0,\ldots,0,0),$$

$$\mathcal{Z}_0^{(3)} = \mathrm{col}(0,0,0,0,0,-i\omega_L/d,1,\ldots,0,0),$$

$$\vdots \tag{17}$$

$$\mathcal{Z}_0^{(N)} = \mathrm{col}(0,0,0,0,0,0,0,\ldots,-i\omega_L/d,1),$$

while those associated with $i\omega_L$ are $\mathcal{Z}_0^{(N+j)}$

$$\mathcal{Z}_0^{(N+j)} = \mathcal{Z}_0^{(j)*} \quad \text{with} \quad j = 2,3,\ldots,N. \tag{18}$$

As for the eigenvalues $-i\omega_R$ and $i\omega_R$, the associated eigenvectors are

$$\mathcal{Z}_0^{(N+1)} = \mathrm{col}(N/(NQ-d), iN\sigma, N, i\sigma, 1, i\sigma, 1, \ldots, i\sigma, 1), \tag{19}$$

where $\sigma = \omega_R/(NQ-d)$ and

$$\mathcal{Z}_0^{(2N+1)} = \mathcal{Z}_0^{(N+1)*}, \tag{20}$$

respectively.

It is easy to verify that the $2N+1$ solutions $\mathcal{Z}_0^{(n)}\exp(\lambda_n T_{-1})$ with $n = 1,2,\ldots,2N+1$ of the homogeneous problem (8) are linearly independent. They thus constitute the fundamental set of solutions of the homogeneous problem and its general solution is

$$\mathcal{Z}_0 = \Phi \cdot A, \tag{21}$$

where Φ is the fundamental matrix of Eq. (8), which is the $(2N+1)\times(2N+1)$ matrix

$$\Phi(T_{-1}) = (\mathcal{Z}_0^{(1)}\exp(\lambda_1 T_{-1}) \quad \mathcal{Z}_0^{(2)}\exp(\lambda_2 T_{-1}) \quad \cdots \quad \mathcal{Z}_0^{(2N+1)}\exp(\lambda_{2N+1} T_{-1})) \tag{22}$$

and A is a $2N+1$ column vector

$$A=\mathrm{col}(A_0,A_{L,1},\ldots,A_{L,N-1},A_R,A_{L,1}^*,\ldots,A_{L,N-1}^*,A_R^*) \tag{23}$$

with A_0 arbitrary real and $A_{L,j}$ and A_R arbitrary complex functions of all the time scales slower than T_{-1}, i.e., of T_0, T_1, etc.

The dependence of the vector A on T_0, T_1, etc. cannot be derived within the $\mathcal{O}(1)$ problem. This is the main restriction of the reference model [2,29] which retains only undamped relaxation oscillations. To get a more complete picture of the laser dynamics, we need to analyze the next order equation (9) which is the $\mathcal{O}(\varepsilon)$ problem.

B. The $\mathcal{O}(\varepsilon)$ problem

Equation (9) is an inhomogeneous equation. Making use of (16)–(20) in (A1), we can express M_1 as

$$\begin{aligned}M_1=M_1^{(0)}+[&M_1^{(L)}\exp(-i\omega_L T_{-1})+M_1^{(R)}\exp(-i\omega_R T_{-1})\\&+M_1^{(2L)}\exp(-2i\omega_L T_{-1})+M_1^{(2R)}\exp(-2i\omega_R T_{-1})\\&+M_1^{(L-R)}\exp[-i(\omega_L-\omega_R)T_{-1}]\\&+M_1^{(L+R)}\exp[-i(\omega_L+\omega_R)T_{-1}]+\text{c.c.}],\end{aligned} \tag{24}$$

where the matrices $M_1^{(j)}$ are given in Appendix B.

Since the homogeneous part of (9) coincides with the homogeneous problem (8) and the inhomogeneous part M_1 contains terms proportional to $\exp(i\omega T_{-1})$ with $\omega=0$, ω_L and ω_R, the problem (9) has bounded and periodic solutions if the following solvability conditions are satisfied [2]:

$$0=[M_1^{(0)},F^{(1)}], \tag{25}$$

$$0=[M_1^{(L)},F^{(N+j)}];\quad j=2,3,\ldots,N, \tag{26}$$

$$0=[M_1^{(R)},F^{(2N+1)}], \tag{27}$$

where $[\alpha,\beta]$ denotes the inner product of α and β while $F^{(n)}$ are the eigenvectors of the homogeneous adjoint problem

$$\frac{\partial F}{\partial T_{-1}}=-L^+F,\quad \langle\alpha,L\beta\rangle\equiv\langle L^+\alpha,\beta\rangle \tag{28}$$

with $\langle\alpha,\beta\rangle$ the scalar product of α and β. The matrix L^+ has the same eigenvalues (11) to (15) as L. Its eigenvectors are

$$F^{(1)}=\mathrm{col}(d-NQ,0,1,0,0,0,0,\ldots,0,0), \tag{29}$$

$$\begin{aligned}F^{(2)}&=\mathrm{col}(0,2i\omega_L/NI,-1/N,-2i\omega_L/I,1,0,0,\ldots,0,0),\\F^{(3)}&=\mathrm{col}(0,2i\omega_L/NI,-1/N,0,0,-2i\omega_L/I,1,\ldots,0,0),\\&\vdots\\F^{(N)}&=\mathrm{col}(0,2i\omega_L/NI,-1/N,0,0,0,0,\ldots,-2i\omega_L/I,1),\end{aligned} \tag{30}$$

$$F^{(N+1)}=\mathrm{col}(-2N,-2i\omega_R/I,1,0,0,0,0,\ldots,0,0), \tag{31}$$

and

$$F^{(N+j)}=F^{(j)*}\quad\text{with}\quad j=2,3,\ldots,N+1. \tag{32}$$

Solving Eq. (9) yields the explicit dependence on T_0 of the functions A

$$A_0=B_0(T_1,T_2,\ldots)\exp(-\Gamma_0T_0) \tag{33}$$

with

$$\Gamma_0=1+N(2N-1)I^2/(2\omega_R^2), \tag{34}$$

$$A_{L,j}=B_{L,j}(T_1,T_2,\ldots)\exp(-\Gamma_LT_0),j=1,2,\ldots,N-1 \tag{35}$$

with

$$\Gamma_L=U/2, \tag{36}$$

and

$$A_R=B_R(T_1,T_2,\ldots)\exp(-\Gamma_RT_0) \tag{37}$$

with

$$\Gamma_R=(2N+1)wI/(4\omega_R^2). \tag{38}$$

In the above formulas the functions B are still arbitrary.

Using (33), (35), and (37), the vector A given by (23) becomes

$$\begin{aligned}A=\mathrm{col}(&B_0\exp(-\Gamma_0T_0),B_{L,1}\exp(-\Gamma_LT_0),\ldots,B_{L,N-1}\\&\times\exp(-\Gamma_LT_0),B_R\exp(-\Gamma_RT_0),B_{L,1}^*\\&\times\exp(-\Gamma_LT_0),\ldots,B_{L,N-1}^*\exp(-\Gamma_LT_0),B_R^*\\&\times\exp(-\Gamma_RT_0)).\end{aligned} \tag{39}$$

The general solution of Eq. (9) is

$$\mathcal{Z}_1=\tilde{\mathcal{Z}}_0+\mathcal{Z}_{1,par},\quad \tilde{\mathcal{Z}}_0=\Phi\cdot\tilde{A} \tag{40}$$

where $\tilde{A}$ is given by Eq. (39) with B replaced by $\tilde{B}$, and $\mathcal{Z}_{1,par}$ is a particular solution of Eq. (9):

$$\mathcal{Z}_{1,par}=\Phi\cdot\int\Phi^{-1}\cdot\tilde{M}_1dT_{-1}. \tag{41}$$

The vector $\tilde{M}_1$ is given by (A1) in which $\mathcal{D}_0$, $\mathcal{I}_{T0}$, $\mathcal{Q}_{T0}$, $\mathcal{I}_{q0}$, and $\mathcal{Q}_{q0}$ are replaced by $\tilde{\mathcal{D}}_0$, $\tilde{\mathcal{I}}_{T0}$, $\tilde{\mathcal{Q}}_{T0}$, $\tilde{\mathcal{I}}_{q0}$, and $\tilde{\mathcal{Q}}_{q0}$, respectively. Substituting Φ from (22) and $\tilde{M}_1$ into (41) yields

$$\begin{aligned}\mathcal{Z}_{1,par}=\mathcal{Z}_{1,par}^{(0)}&\exp(-\Gamma_0T_0)+\{\mathcal{Z}_{1,par}^{(L)}\exp(-i\omega_LT_{-1}-\Gamma_LT_0)\\&+\mathcal{Z}_{1,par}^{(R)}\exp(-i\omega_RT_{-1}-\Gamma_RT_0)\\&+\mathcal{Z}_{1,par}^{(2L)}\exp(-2i\omega_LT_{-1}-2\Gamma_LT_0)\\&+\mathcal{Z}_{1,par}^{(2R)}\exp(-2i\omega_RT_{-1}-2\Gamma_RT_0)+\mathcal{Z}_{1,par}^{(L-R)}\\&\times\exp[-i(\omega_L-\omega_R)T_{-1}-(\Gamma_L+\Gamma_R)T_0]+\mathcal{Z}_{1,par}^{(L+R)}\\&\times\exp[-i(\omega_L+\omega_R)T_{-1}-(\Gamma_L+\Gamma_R)T_0]+\text{c.c.}\}.\end{aligned}$$

The different components of $\mathcal{Z}_{1,par}$ are

$$\mathcal{Z}_{1,par}^{(0)}=\frac{(2N-1)I\tilde{B}_0}{2[d-N(Q-2)]}\mathrm{col}(0,N,0,1,0,1,0,\ldots,1,0), \tag{42}$$

$$\mathcal{Z}^{(L)}_{1,par}=\frac{U}{4d}\mathrm{col}\left(0,0,0,\widetilde{B}_{L,1},\frac{-id\widetilde{B}_{L,1}}{\omega_L},\widetilde{B}_{L,2},\frac{-id\widetilde{B}_{L,2}}{\omega_L},\ldots,\widetilde{B}_{L,N-1},\frac{-id\widetilde{B}_{L,N-1}}{\omega_L}\right), \tag{43}$$

$$\mathcal{Z}^{(R)}_{1,par}=\frac{\widetilde{B}_R}{4[N(Q-2)-d](NQ-d)}\mathrm{col}(Ni\alpha,N\beta,Ni\vartheta,\beta,i\vartheta,\beta,i\vartheta,\ldots,\beta,i\vartheta), \tag{44}$$

$$\mathcal{Z}^{(2L)}_{1,par}=\frac{Nb}{I(4\omega_L^2-\omega_R^2)}\mathrm{col}(i\widetilde{B}_L^2,-2\omega_L\widetilde{B}_L^2,i(NQ-d)\widetilde{B}_L^2,\varphi_1,i\phi_1,\varphi_2,i\phi_2,\ldots,\varphi_{N-1},i\phi_{N-1}), \tag{45}$$

$$\mathcal{Z}^{(2R)}_{1,par}=\frac{g\widetilde{B}_R^2}{6I\omega_R^2}\mathrm{col}(Ni,-2N\omega_R,Ni(NQ-d),\chi,\eta,\chi,\eta,\ldots,\chi,\eta), \tag{46}$$

$$\mathcal{Z}^{(L-R)}_{1,par}=\frac{d\omega^{(-)}h^{(-)}\widetilde{B}_R^*}{\omega_R(2\omega_L-\omega_R)}\mathrm{col}\left(0,0,0,\widetilde{B}_{L,1},\frac{i\widetilde{B}_{L,1}}{\omega^{(-)}},\widetilde{B}_{L,2},\frac{i\widetilde{B}_{L,2}}{\omega^{(-)}},\ldots,\widetilde{B}_{L,N-1},\frac{i\widetilde{B}_{L,N-1}}{\omega^{(-)}}\right), \tag{47}$$

and

$$\mathcal{Z}^{(L+R)}_{1,par}=\frac{d\omega^{(+)}h^{(+)}\widetilde{B}_R}{\omega_R(2\omega_L+\omega_R)}\mathrm{col}\left(0,0,0,\widetilde{B}_{L,1},\frac{i\widetilde{B}_{L,1}}{\omega^{(+)}},\widetilde{B}_{L,2},\frac{i\widetilde{B}_{L,2}}{\omega^{(+)}},\ldots,\widetilde{B}_{L,N-1},\frac{i\widetilde{B}_{L,N-1}}{\omega^{(+)}}\right). \tag{48}$$

The notation used in the above formulas is defined in Appendix C.

With this, we have determined the explicit dependence of the dynamical variables on the first two time scales, T_{-1} and T_0. Information on the slower time scales $T_1,T_2,\ldots$ is contained in the functions $\widetilde{B}$.

C. The $\mathcal{O}(\varepsilon^2)$ problem

The unknown functions $\widetilde{B}$ should, in turn, be determined by analyzing the $\mathcal{O}(\varepsilon^2)$ problem, Eq. (10). This problem admits periodic solutions provided that its inhomogeneous part obeys the solvability conditions

$$0=[\widetilde{M}_2^{(0)},F^{(1)}], \tag{49}$$

$$0=[\widetilde{M}_2^{(L)},F^{(N+j)}];\quad j=2,3,\ldots,N, \tag{50}$$

$$0=[\widetilde{M}_2^{(R)},F^{(2N+1)}]. \tag{51}$$

The $\widetilde{M}_2^{(0,L,R)}$ which are defined in Appendix D, are related to $\widetilde{M}_2$ as follows:

$$\widetilde{M}_2=\widetilde{M}_2^{(0)}\exp(-\Gamma_0T_0)+[\widetilde{M}_2^{(L)}\exp(-\Gamma_LT_0-i\omega_LT_{-1}) + \widetilde{M}_2^{(R)}\exp(-\Gamma_RT_0-i\omega_RT_{-1})+\mathrm{NST's+c.c.}], \tag{52}$$

where NST denotes nonsecular term and the matrices $\widetilde{M}_2^{(j)}$ are given in Appendix D.

The solvability conditions (49)–(51) yield

$$\widetilde{B}_0=C_0\exp(-g_0T_1), \tag{53}$$

$$\widetilde{B}_{L,j}=C_{L,j}\exp(-g_LT_1), \tag{54}$$

$$\widetilde{B}_R=C_R\exp[(i\rho_R-g_R)T_1], \tag{55}$$

where the C's are unknown functions of $T_2,T_3,\ldots$, while

$$g_0=\frac{d-1}{\omega_R^2}-\Gamma_0=-\frac{NI}{\omega_R^2}\left[1+\left(N-\frac{1}{2}\right)I\right], \tag{56}$$

$$g_L=-\Gamma_L, \tag{57}$$

$$g_R=\frac{NIw}{2\omega_R^2}-\Gamma_R=-\frac{Iw}{4\omega_R^2} \tag{58}$$

and

$$\rho_R=\frac{I}{2\omega_R^2}\left\{\frac{1}{8\omega_R}\left[\frac{NI\alpha(w-\Gamma_R)}{\omega_R}+\beta\Gamma_R\right]-Nw\omega_R\right\}.$$

D. Initial conditions

So far we have derived the dependence of the solution on T_{-1}, T_0, and T_1. Because the slower time scales T_2, T_3, ... are not of practical importance, we can complete our analysis by determining the still unknown quantities B and C from the initial condition, which should also be expanded in powers of ε,

$$\mathcal{Z}^0=\varepsilon(\mathcal{Z}_0^0+\varepsilon\mathcal{Z}_1^0+\cdots),$$

where the superscript implies the initial value of the dynamical variable. Obviously, the B's are to be obtained from

$$\mathcal{Z}_0(0,0,\ldots)=\mathcal{Z}_0^0 \tag{59}$$

and the C's from

$$\mathcal{Z}_1(0,0,\ldots)=\mathcal{Z}_1^0, \tag{60}$$

where $\mathcal{Z}_0(0,0,\ldots)$ and $\mathcal{Z}_1(0,0,\ldots)$ are given by Eqs. (21) and (40), respectively. We shall only solve Eq. (59), since it provides the dominant behavior of the laser dynamics. In matrix form, Eq. (59) reads

$$\mathcal{M}\mathcal{B}=\mathcal{Z}_0^0, \tag{61}$$

where

$$\mathcal{M}=\begin{pmatrix}
\frac{1}{2} & 0 & 0 & \cdots & 0 & -\frac{NI}{2(d-1)} & 0 & 0 & \cdots & 0 & -\frac{NI}{2(d-1)} \\
0 & 0 & 0 & \cdots & 0 & -\frac{iNI\omega_R}{2(d-1)} & 0 & 0 & \cdots & & \frac{iNI\omega_R}{2(d-1)} \\
N & 0 & 0 & \cdots & 0 & N & 0 & 0 & \cdots & 0 & N \\
0 & -\frac{i\omega_L}{d} & 0 & \cdots & 0 & -\frac{iI\omega_R}{2(d-1)} & \frac{i\omega_L}{d} & 0 & \cdots & 0 & \frac{iI\omega_R}{2(d-1)} \\
1 & 1 & 0 & \cdots & 0 & 1 & 1 & 0 & \cdots & 0 & 1 \\
0 & 0 & -\frac{i\omega_L}{d} & \cdots & 0 & -\frac{iI\omega_R}{2(d-1)} & 0 & \frac{i\omega_L}{d} & \cdots & 0 & \frac{iI\omega_R}{2(d-1)} \\
1 & 0 & 1 & \cdots & 0 & 1 & 0 & 1 & \cdots & 0 & 1 \\
\vdots & \vdots & \vdots & \ddots & \vdots & \vdots & \vdots & \vdots & \ddots & \vdots & \vdots \\
0 & 0 & 0 & \cdots & -\frac{i\omega_L}{d} & -\frac{iI\omega_R}{2(d-1)} & 0 & 0 & \cdots & \frac{i\omega_L}{d} & \frac{iI\omega_R}{2(d-1)} \\
1 & 0 & 0 & \cdots & 1 & 1 & 0 & 0 & \cdots & 1 & 1
\end{pmatrix},$$

$$\mathcal{B}=\mathrm{col}(B_0,B_{L,1},B_{L,2},\ldots,B_{L,N-1},B_R,B_{L,1}^*,B_{L,2}^*,\ldots,B_{L,N-1}^*,B_R^*),$$

and

$$\mathcal{Z}_0^0=\mathrm{col}(\mathcal{D}_0^0,\mathcal{I}_{T0}^0,\mathcal{Q}_{T0}^0,\mathcal{I}_{20}^0,\mathcal{Q}_{20}^0,\mathcal{I}_{30}^0,\mathcal{Q}_{30}^0,\ldots,\mathcal{I}_{N0}^0,\mathcal{Q}_{N0}^0).$$

Solving Eq. (61) yields at once an explicit expression of the B's in terms of the initial condition

$$B_0=\frac{I\mathcal{Q}_{T0}^0+2(d-1)\mathcal{D}_0^0}{\omega_R^2}, \tag{62}$$

$$B_{L,q-1}=\frac{N\mathcal{Q}_{q0}^0-\mathcal{Q}_{T0}^0}{2N}+i\frac{d(N\mathcal{I}_{q0}^0-\mathcal{I}_{T0}^0)}{2N\omega_L} \tag{63}$$

for $q=2,3,\ldots,N$, and

$$B_R=\frac{(d-1)(\mathcal{Q}_{T0}^0-2N\mathcal{D}_0^0)}{2N\omega_R^2}+i\frac{(d-1)\mathcal{I}_{T0}^0}{NI\omega_R}. \tag{64}$$

IV. DISCUSSION

Having solved the nonlinear problem analytically in a perturbative manner, we discuss in this section the physical consequences of our results: intensity coherence, damping rates, and universal versus initial-condition-sensitive properties.

A. Intensity coherence

The collective self-organized feature of multimode Fabry-Perot lasers is that relaxation oscillations of the modal intensities are not uncorrelated. At both $\mathcal{O}(1)$ and $\mathcal{O}(\varepsilon)$, modal oscillations at Ω_R are always inphased because the coefficients of $\exp(\pm i\omega_R T_{-1})$ for the total intensity are precisely N times those for a modal intensity, as is clearly seen from Eqs. (19) and (44). On the other hand, for oscillations at Ω_L, perfect antiphase occurs at both $\mathcal{O}(1)$ and $\mathcal{O}(\varepsilon)$ because the modal intensities contain terms proportional to $\exp(\pm i\omega_L T_{-1})$, while the total intensity has no contribution proportional to $\exp(\pm i\omega_L T_{-1})$, as is clearly seen from Eqs. (17) and (43).

The additional signature of AD gained from the nonlinear analysis developed in this paper is that at $\mathcal{O}(\varepsilon)$ the oscillation at $\Omega_R\pm\Omega_L$ is present in the modal intensities but absent in the total intensity, as is clearly seen from Eqs. (47) and (48). Thus, perfect antiphase arises at $\Omega_R\pm\Omega_L$ as well. Our analytical results are confirmed numerically in Fig. 1, where we plot the intensity power spectra using the transient time evolution obtained by numerically solving the full nonlinear TSD equations (1). It is evident from Fig. 1 that, in order of increasing frequencies, there are six peaks at Ω_L, $\Omega_R-\Omega_L$,

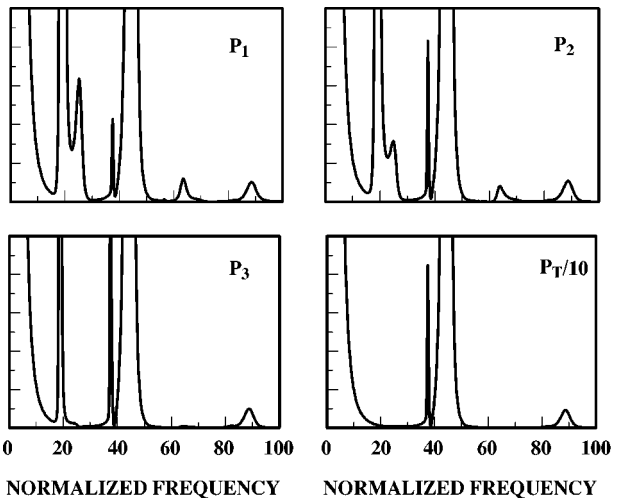

FIG. 1. Intensity power spectra calculated numerically from the full nonlinear TSD equations (1) for $N=3$, $k=5\times10^4$, and equal modal gains. The laser is initially near the steady state corresponding to the pump $w_0=4.6$. The initial condition is $D^0=d(w_0)$, $Q_q^0=Q(w_0)[1+0.01/(q+1)]$, and $I_q^0=I(w_0)[1+0.01/(q+N+1)]$. The final state is the steady state with $w=2.6$. Up to $\mathcal{O}(\varepsilon)$, our theory gives six possible oscillation frequencies: $\Omega_L\simeq18.69$, $\Omega_R-\Omega_L\simeq26.33$, $2\Omega_L\simeq37.37$, $\Omega_R\simeq45.02$, $\Omega_R+\Omega_L\simeq63.70$, and $2\Omega_R\simeq90.03$, which are well reproduced in the power spectra of the modal intensities. The total intensity power spectrum, as predicted by the theory, displays only three peaks at $2\Omega_L$, Ω_R, and $2\Omega_R$. Perfect antiphase at $\Omega_R\pm\Omega_L$, in addition to that at Ω_L, is verified. For all figures, frequencies are in units of the population inversion decay rate.

$2\Omega_L$, Ω_R, $\Omega_R+\Omega_L$, and $2\Omega_R$ in the power spectra of the modal intensities but only three peaks at $2\Omega_L$, Ω_R, and $2\Omega_R$ in that of the total intensity.

B. Damping rates

A nonlinear analysis is essential in obtaining the dependence on time scales slower than T_{-1}. From the solvability conditions (25)–(27) we obtain the dependence on T_0 at $\mathcal{O}(\epsilon)$, which is of the form $\exp(-\Gamma_{0,L,R}T_0)$, as seen in Eqs. (33), (35), and (37). Of importance is the fact that we have been able to derive the Γ's, Eqs. (34), (36), and (38), in such a way that their positivity is manifest. This reveals that at $\mathcal{O}(\epsilon)$ the relaxation oscillations decay in time and the Γ's are the damping rates. Furthermore, a direct use of Eqs. (34), (36), and (38) yields the relation between the different damping rates [35]

$$\Gamma_0=2(2\Gamma_L-\Gamma_R), \tag{65}$$

from which it follows that

$$\Gamma_L>\frac{1}{2}\Gamma_R.$$

However, more interesting is the relative magnitude between Γ_L and Γ_R themselves (rather than between Γ_L and $\Gamma_R/2$). This can be obtained by observing, from Eqs. (36) and (38), that

$$\Gamma_R-\Gamma_L=\frac{NI[I+2(d-1)]}{4\omega_R^2}. \tag{66}$$

Obviously, the rhs of Eq. (66) is positive and, hence, we have the relation

$$\Gamma_R>\Gamma_L, \tag{67}$$

which means that the oscillation at Ω_R decays faster than the oscillation at Ω_L.

The dependence on T_1 displayed by $\tilde{B}_0$, $\tilde{B}_{L,j}$, and $\tilde{B}_R$ in Eqs. (53), (54), and (55) is derived from the solvability conditions (49)–(51). It is obvious, from (56)–(58), that g_0, g_L, and g_R are all real and negative. Furthermore, it is easily checked from (56)–(58), that the absolute values of the g's are bounded

$$|g_0|<\Gamma_0, \quad |g_L|=\Gamma_L \quad \text{and} \quad |g_R|<\Gamma_R, \tag{68}$$

guaranteeing stability of the steady state up to $\mathcal{O}(\varepsilon^2)$. At this order of approximation the damping rates of the oscillations at Ω_L, $\Omega_R\pm\Omega_L$, $2\Omega_L$, Ω_R, and $2\Omega_R$ are, respectively, $\mathcal{G}_L=\Gamma_L+\varepsilon g_0$, $\mathcal{G}_{R\pm L}=\Gamma_R+\Gamma_L+\varepsilon(g_R+g_L)$, $\mathcal{G}_{2L}=2\mathcal{G}_L=2(\Gamma_L+\varepsilon g_L)$, $\mathcal{G}_R=\Gamma_R+\varepsilon g_R$, and $\mathcal{G}_{2R}=2\mathcal{G}_R=2(\Gamma_R+\varepsilon g_R)$. It follows from Eq. (68) that the damping rates $\mathcal{G}$ are all positive.

It is interesting to note the relationship between the g's,

$$g_0=2(g_L-g_R), \tag{69}$$

from which we readily get

$$g_R>g_L. \tag{70}$$

Relation (69) is easily derived from (65) by taking into account Eqs. (56)–(58) and the equalities $w=\omega_R^2+1$ as well as $\omega_R^2=NI+d-1$. Relations (67) and (70) allow us to remark that up to $\mathcal{O}(\varepsilon^2)$ the oscillation at Ω_R is still damped out faster than the oscillation at Ω_L because

$$\mathcal{G}_R-\mathcal{G}_L=\Gamma_R-\Gamma_L+\varepsilon(g_R-g_L)>0.$$

C. Universal versus initial-condition-sensitive properties

An effective tool to study the laser dynamics is the intensity power spectrum defined by

$$P_j(\Omega)=\left|\int_0^\infty \mathcal{I}_j(t)\exp(2\pi i\Omega t)dt\right|^2, \tag{71}$$

where $j=T$ corresponds to the total intensity and $j=q$ to mode q intensity. It is clear from our analytical results, Eqs. (17), (19), (43), (44), (47), and (48) that, independent of the initial condition, the following power spectra relations hold:

$$P_1(\Omega_R)=P_2(\Omega_R)=\cdots=P_N(\Omega_R),$$

$$P_T(\Omega_R)=N^2P_p(\Omega_R); \quad p=1,2,\ldots,N, \tag{72}$$

$$P_T(\Omega_L)=P_T(\Omega_R+\Omega_L)=P_T(\Omega_R-\Omega_L)=0.$$

The above relations are an expression of the inphased dynamics at Ω_R and the perfect antiphase at Ω_L and $\Omega_R \pm \Omega_L$. These properties are universal in the sense that they depend neither on the initial conditions nor on the laser parameters.

On the contrary, the power spectrum peak height at a certain frequency is a function of the initial condition. While the peak height at $2\Omega_L$, $2\Omega_R$, and $\Omega_R \pm \Omega_L$ is entirely dictated by the C coefficients the peaks at Ω_L and Ω_R are mainly determined by the B coefficients. The correction to $P_q(\Omega_{L,R})$ due to the C's is a small correction of order ε. Since the explicit dependence of the B's on the initial condition has been derived in Eqs. (62)–(64), we are in a position to investigate $P_q(\Omega_{L,R})$ as a function of the initial condition. Making use of Eqs. (62)–(64) we write the modal intensity to leading order of ε in the form

$$\mathcal{I}_q(t) = [\alpha_R \cos(2\pi\Omega_R t) + \beta_R \sin(2\pi\Omega_R t)]\exp(-\Gamma_R t) + [\alpha_{L,q}\cos(2\pi\Omega_L t) + \beta_{L,q}\sin(2\pi\Omega_L t)]\exp(-\Gamma_L t), \tag{73}$$

where

$$\alpha_R = \frac{\mathcal{I}^0_{T0}}{N}, \quad \beta_R = \frac{I(2N\mathcal{D}^0_0 - \mathcal{Q}^0_{T0})}{2N\omega_R},$$

$$\alpha_{L,q} = \frac{N\mathcal{I}^0_{q0} - \mathcal{I}^0_{T0}}{N}, \quad \text{and} \quad \beta_{L,q} = \frac{\omega_L(\mathcal{Q}^0_{T0} - N\mathcal{Q}^0_{q0})}{Nd}.$$

Inserting Eq. (73) into Eq. (71) and integrating over t, we readily obtain

$$P_q(\Omega_R) = 4\pi^2\Omega_R^2\left\{\frac{\alpha_R\Gamma_R + 4\pi\beta_R\Omega_R}{\Gamma_R(\Gamma_R^2 + 16\pi^2\Omega_R^2)} + \frac{4\pi\beta_{L,q}\Gamma_L\Omega_L + \alpha_{L,q}[\Gamma_L^2 + 4\pi^2(\Omega_R^2 - \Omega_L^2)]}{[\Gamma_L^2 + 4\pi^2(\Omega_R+\Omega_L)^2][\Gamma_L^2 + 4\pi^2(\Omega_R-\Omega_L)^2]}\right\}^2 + \left\{\frac{\alpha_R(\Gamma_R^2 + 8\pi^2\Omega_R^2) + 2\pi\beta_R\Gamma_R\Omega_R}{\Gamma_R(\Gamma_R^2 + 16\pi^2\Omega_R^2)} + \frac{2\pi\beta_{L,q}\Omega_L[\Gamma_L^2 - 4\pi^2(\Omega_R^2 - \Omega_L^2)] + \alpha_{L,q}\Gamma_L[\Gamma_L^2 + 4\pi^2(\Omega_R^2 + \Omega_L^2)]}{[\Gamma_L^2 + 4\pi^2(\Omega_R+\Omega_L)^2][\Gamma_L^2 + 4\pi^2(\Omega_R-\Omega_L)^2]}\right\}^2 \tag{74}$$

and

$$P_q(\Omega_L) = P_q(\Omega_R)\big|_{\{\Gamma_R \leftrightarrow \Gamma_L, \Omega_R \leftrightarrow \Omega_L, \alpha_R \leftrightarrow \alpha_{L,q}, \beta_R \leftrightarrow \beta_{L,q}\}}. \tag{75}$$

In our theory, by definition, $\Omega_{L,R}$ are $\mathcal{O}(\varepsilon^{-1})$ and $\Gamma_{L,R}$ are $\mathcal{O}(1)$, i.e., $\Omega_{L,R} \gg \Gamma_{L,R}$. In this limit, Eqs. (74) and (75) reduce to

$$P_q(\Omega_R) \simeq \frac{\alpha_R^2 + \beta_R^2}{4\Gamma_R^2} = \frac{(2\omega_R\mathcal{I}^0_{T0})^2 + I^2(2N\mathcal{D}^0_0 - \mathcal{Q}^0_{T0})^2}{16N^2\omega_R^2\Gamma_R^2} \forall q \tag{76}$$

and

$$P_q(\Omega_L) \simeq \frac{\alpha_{L,q}^2 + \beta_{L,q}^2}{4\Gamma_L^2} = \frac{d^2(N\mathcal{I}^0_{q0} - \mathcal{I}^0_{T0})^2 + \omega_L^2(\mathcal{Q}^0_{T0} - N\mathcal{Q}^0_{q0})^2}{4N^2d^2\Gamma_L^2}. \tag{77}$$

Now we are able to relate power spectrum peak heights not only at the same frequency but also at different frequencies. As a consequence of Eqs. (76) and (77), we can make the following remarks.

(1) The peak height at Ω_R is mode independent and is determined by the initial deviations $\mathcal{D}^0_0$, $\mathcal{Q}^0_{T0}$, and $\mathcal{I}^0_{T0}$ of the global variables only.

(2) The peak height at Ω_L is mode dependent and is unaffected by the initial deviation of the spatially averaged population inversion $\mathcal{D}^0_0$. AD at Ω_L is a very sensitive function of the initial conditions: (i) All modes may have a finite peak $P_q(\Omega_L) > 0$ if $\mathcal{Q}^0_{q0} \neq \mathcal{Q}^0_{T0}/N$ or/and $\mathcal{I}^0_{q0} \neq \mathcal{I}^0_{T0}/N$ for all q. In particular, if $\mathcal{Q}^0_{q0}$ and $\mathcal{I}^0_{q0}$ are such that $\mathcal{Q}^0_{T0} = \mathcal{I}^0_{T0} = 0$, then $P_q(\Omega_L) \propto (\omega_L\mathcal{Q}^0_{q0})^2 + (d\mathcal{I}^0_{q0})^2$. Figure 2 displays the power spectra for $N=3$, $k = 5\times10^4$ and the initial conditions $\mathcal{D}^0_0 = 3.5$, $\mathcal{Q}^0_{10} = 3.0$, $\mathcal{Q}^0_{20} = -2.0$, $\mathcal{Q}^0_{30} = -1.0$, $\mathcal{I}^0_{10} = 2.0$, $\mathcal{I}^0_{20} = -1.1$, and $\mathcal{I}^0_{30} = -0.9$. These power spectra are obtained by numerical simulation of the full TSD rate equations (1). According to Eq. (77), our theory predicts $P_1(\Omega_L) > P_2(\Omega_L) > P_3(\Omega_L) > 0$. Indeed, this is numerically confirmed in Fig. 2. The fact that perfect antiphase occurs when every mode has a nonzero power spectrum peak cannot be obtained from the analysis based only on the eigenvector: the initial condition plays a crucial role. (ii) A mode q displays no peak, i.e., $P_q(\Omega_L) = 0$, if its initial deviations satisfy the conditions $\mathcal{Q}^0_{q0} = \mathcal{Q}^0_{T0}/N$ and $\mathcal{I}^0_{q0} = \mathcal{I}^0_{T0}/N$. If there are $N-2$ such modes, then the two remaining modes have equal peaks regardless of their initial states. This is illustrated numerically in Fig. 3 for $N=3$, $k = 5\times10^4$, $\mathcal{D}^0_0 = 0.1$, $\mathcal{Q}^0_{10} = 9.0$, $\mathcal{Q}^0_{20} = 1.0$, $\mathcal{Q}^0_{30} = 5.0$, $\mathcal{I}^0_{10} = 10.0$, $\mathcal{I}^0_{20} = 2.0$, and $\mathcal{I}^0_{30} = 6.0$. (iii) Depending on the initial condition, a special situation may occur in which all the individual modal intensities as well as the total intensity show only one peak at Ω_R but no peak at

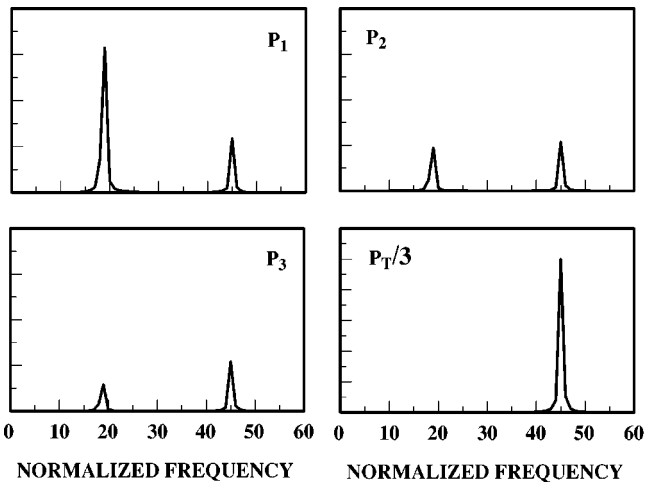

FIG. 2. Same as Fig. 1 but the initial state is specified by $D^0=d(w)+3.5/k$, $Q_1^0=Q(w)+3.0/k$, $Q_2^0=Q(w)-2.0/k$, $Q_3^0=Q(w)-1.0/k$, $I_1^0=I(w)+2.0/\sqrt{k}$, $I_2^0=I(w)-1.1/\sqrt{k}$, and $I_3^0=I(w)-0.9/\sqrt{k}$. The peak relations $P_1(\Omega_L)>P_2(\Omega_L)>P_3(\Omega_L)>0$ and $P_1(\Omega_R)=P_2(\Omega_R)=P_3(\Omega_R)>0$ agree with the analytical result.

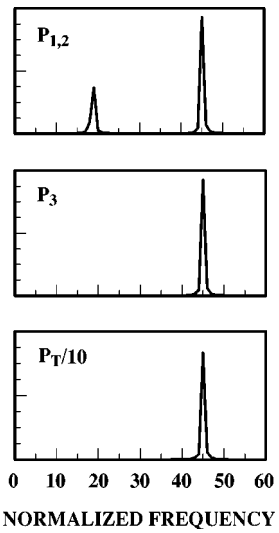

FIG. 3. Same as in Fig. 2 but $D^0=d(w)+0.1/k$, $Q_1^0=Q(w)+9.0/k$, $Q_2^0=Q(w)+1.0/k$, $Q_3^0=Q(w)+5.0/k$, $I_1^0=I(w)+10.0/\sqrt{k}$, $I_2^0=I(w)+2.0/\sqrt{k}$, and $I_3^0=I(w)+6.0/\sqrt{k}$. At Ω_L mode 3 displays no peak while modes 1 and 2 show equal peaks, in accordance with the theory.

all at Ω_L. Theoretically, this corresponds to the ''symmetric'' initial conditions $\{\mathcal{Q}_{10}^0=\mathcal{Q}_{20}^0=\cdots=\mathcal{Q}_{N0}^0$ and $\mathcal{I}_{10}^0=\mathcal{I}_{20}^0=\cdots=\mathcal{I}_{N0}^0\}$. This is confirmed numerically in Fig. 4.

(3) The modal peak ratio at different frequencies, as a rule, depends strongly on the initial condition. In Fig. 5, again for $N=3$, $k=5\times10^4$, we draw the ratio $R_q=P_q(\Omega_L)/P_q(\Omega_R)$ as a function of $\mathcal{D}_0^0$ and fixed $\mathcal{Q}_{10}^0=3.0$, $\mathcal{Q}_{20}^0=-2.0$, $\mathcal{Q}_{30}^0=-1.0$, $\mathcal{I}_{10}^0=2.0$, $\mathcal{I}_{20}^0=-1.1$, and $\mathcal{I}_{30}^0=-0.9$. The agreement between the theoretical (solid curves) and numerical (black circles) results is very good. Note again that without considering the initial condition, no relations between the power spectrum peak heights at different frequencies can be established.

V. THE RESONANT CASE

The analytic results presented above are invalid for $\Omega_R=2\Omega_L$ since this makes both $\mathcal{Z}_{1,par}^{(2L)}$ in Eq. (45) and $\mathcal{Z}_{1,par}^{(L-R)}$ in Eq. (47) divergent. Solving the implicit equation $\Omega_R=2\Omega_L$ yields $N=2$ and $w=15/7$ [2,11]. This resonant case must be handled separately. The $\mathcal{O}(1)$ general solution remains formally determined by (21) but the amplitudes A_L, A_R do not simply follow the laws (35), (37). Instead of Eq. (24), the resonant case requires the following decomposition of M_1:

$$M_1=M_1^{(0)}+[M_1^{(1)}\exp(-i\omega_L T_{-1})+M_1^{(2)}\exp(-2i\omega_L T_{-1})+M_1^{(3)}\exp(-3i\omega_L T_{-1})+M_1^{(4)}\exp(-4i\omega_L T_{-1})+\text{c.c.}], \tag{78}$$

where $\omega_L=\omega_R/2=\sqrt{2/7}$ and $M_1^{(0,1,2,3,4)}$ are given in Appendix E.

The solvability conditions (25)–(27) with $M_1^{(0)}$, $M_1^{(L)}\equiv M_1^{(1)}$, and $M_1^{(R)}\equiv M_1^{(2)}$ yield that the amplitude A_0 must vary in T_0 as

$$A_0=B_0(T_1,T_2,\ldots)\exp(-53T_0/32)$$

with $B_0(T_1,T_2,\ldots)$ an unknown function, whereas the T_0-dependent A_L and A_R verify two coupled differential equations

$$\dot{A}_L=-A_L+A_L^*A_R,$$

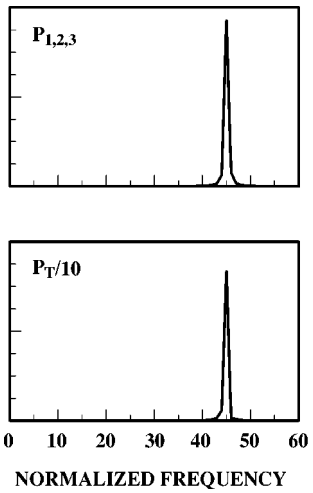

FIG. 4. Same as Fig. 2 but the individual modes are equally perturbed at $t=0$: $D^0=d(w)+1.0/k$, $Q_{1,2,3}^0=Q(w)+3.0/k$, and $I_{1,2,3}^0=I(w)+2.0/\sqrt{k}$. Both analytical and numerical results yield no peaks at Ω_L in the power spectra of both the modal and total intensities.

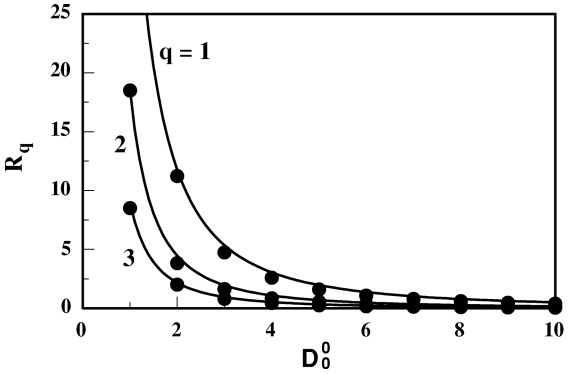

FIG. 5. The ratios $R_q = P_q(\Omega_L)/P_q(\Omega_R)$ between the power spectrum peak heights at different frequencies as a function of $\mathcal{D}_0^0$ when the other initial values are fixed as $Q_1^0 = Q(w) + 3.0/k$, $Q_2^0 = Q(w) - 2.0/k$, $Q_3^0 = Q(w) - 1.0/k$, $I_1^0 = I(w) + 2.0/\sqrt{k}$, $I_2^0 = I(w) - 1.1/\sqrt{k}$, and $I_3^0 = I(w) - 0.9/\sqrt{k}$. The solid curves are plotted using Eqs. (76) and (77), whereas the black circles result from numerical simulations.

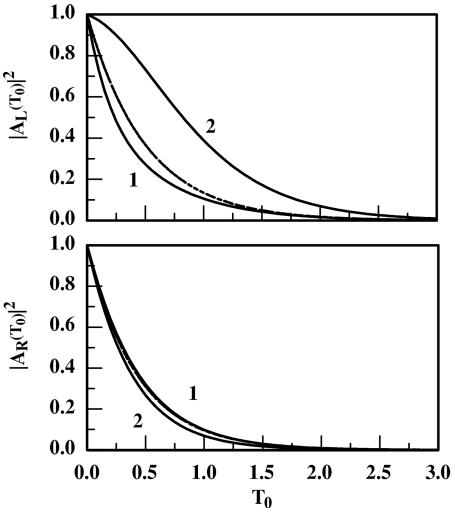

FIG. 6. $|A_L(T_0)|^2$ and $|A_R(T_0)|^2$ vs T_0 for $|A_L(0)|^2 = |A_R(0)|^2 = 1$, $\mathrm{Re}[A_L(0)] = 0.2$, $\mathrm{Re}[A_R(0)] = 0.9$ (curves labeled 1) and $\mathrm{Re}[A_L(0)] = 0.9$, $\mathrm{Re}[A_R(0)] = 0.2$ (curves labeled 2). The dashed curves are for $w \neq 15/7$. The dimensionless time T_0 is defined in Eq. (4).

$$\dot{A}_R = -75A_R/64 - A_L^2/8. \tag{79}$$

These are the usual equations that describe second harmonic generation in nonlinear optics [2]. It is easy to check from Eq. (79) that

$$\frac{\partial}{\partial T_0}\left(|A_R|^2 + \frac{1}{8}|A_R|^2\right) = -\frac{1}{4}\left(\frac{75}{8}|A_R|^2 + |A_R|^2\right) < 0. \tag{80}$$

Equation (80) means that both the Ω_L and Ω_R relaxation oscillations always decay on the time scale T_0 although the corresponding damping rates are not simply 1 and 75/64 as derived for $w \neq 15/7$. Figure 6 illustrates how the decay processes occur and how they are influenced by the initial conditions.

The $\mathcal{O}(\varepsilon)$ particular solution of Eq. (9) in the resonant case is

$$\begin{aligned}\mathcal{Z}_{1,par} = {} & \mathcal{Z}_{1,par}^{(0)}\exp(-53T_0/32) + [\mathcal{Z}_{1,par}^{(1)}\exp(-i\omega_L T_{-1}) \\ & + \mathcal{Z}_{1,par}^{(2)}\exp(-2i\omega_L T_{-1}) + \mathcal{Z}_{1,par}^{(3)}\exp(-3i\omega_L T_{-1}) \\ & + \mathcal{Z}_{1,par}^{(4)}\exp(-4i\omega_L T_{-1}) + \text{c.c.}],\end{aligned}$$

where

$$\mathcal{Z}_{1,par}^{(0)} = \frac{21B_0}{128}\mathrm{col}(0,2,0,1,0),$$

$$\mathcal{Z}_{1,par}^{(1)} = \frac{1}{2}(A_L + A_L^* A_R)\mathrm{col}\left(0,0,0,\frac{7}{8},-i\sqrt{\frac{7}{2}}\right), \tag{81}$$

$$\begin{aligned}\mathcal{Z}_{1,par}^{(2)} = {} & \frac{1}{1536}\mathrm{col}\left(3i\sqrt{\frac{7}{2}}(345A_R - 56A_L^2), 42(75A_R - 8A_L^2),\right. \\ & -12i\sqrt{\frac{7}{2}}(255A_R - 8A_L^2), 35(45A_R + 8A_L^2), \\ & \left.-2i\sqrt{\frac{7}{2}}(765A_R - 152A_L^2)\right),\end{aligned} \tag{82}$$

$$\mathcal{Z}_{1,par}^{(3)} = -\frac{3}{4}A_L A_R \mathrm{col}\left(0,0,0,\frac{21}{8},i\sqrt{\frac{7}{2}}\right), \tag{83}$$

$$\mathcal{Z}_{1,par}^{(4)} = -\frac{7}{3}A_R^2 \mathrm{col}\left(-i\sqrt{\frac{7}{2}},4,2i\sqrt{\frac{2}{7}},2,i\sqrt{\frac{2}{7}}\right). \tag{84}$$

The vectors $\mathcal{Z}$ are five-dimensional, since $N = 2$. The surprising result due to the resonant interaction between the two intrinsic frequencies Ω_L and $\Omega_R = 2\Omega_L$ is that, no matter what A_L and A_R are, the modal oscillations appear to be inphased at $2\Omega_R$ [see Eq. (84)] and *not* at Ω_R as in the nonresonant case. At Ω_R, as is evident from Eq. (82), the inphased dynamics is destroyed by spontaneous subharmonic conversion associated with terms $\propto A_L^2$. It is worth emphasizing that such unusual properties, i.e., inphased oscillations at $2\Omega_R$ but *not* at Ω_R, are specific for the resonant case: any deviation from the resonant case (say, by setting $N = 2$ and $w \neq 15/7$ or $N \geq 3$ and arbitrary $w > 1$) will recover the inphased dynamics at Ω_R and remove it at $2\Omega_R$. As for AD, the resonant case, as revealed from Eqs. (81) and (83), is just a particular case of the general consideration. Here, because of $\Omega_R - \Omega_L = \Omega_L$ and $\Omega_R + \Omega_L = 3\Omega_L$, AD arises at Ω_L and $3\Omega_L$.

VI. CONCLUSION

In this paper we have shown that a multiple time scale analysis of the TSD rate equations can be carried out beyond the usual linear approximation that defines the reference models [29] and [31]. The analysis we have presented is applicable to homogeneously broadened Fabry-Perot lasers characterized by a photon lifetime much smaller than the fluorescence lifetime. This limit holds for many solid-state and microchip lasers. Without any approximation, the TSD equations are not solvable in analytic form for an arbitrary number of modes. We have introduced two simplifying assumptions that make the problem soluble by iteration: the linear gains and losses are mode independent. This is a standard approximation and its validity rests on the fact that the longitudinal modes are spread over a very small fraction of the linear gains and losses of the spectral ranges.

The mathematical development is presented in Sec. III, while the physical consequences are discussed in Sec. IV. Among the results obtained here is the list of frequencies at which the solution of the TSD equations will display oscillations and the relative weight of these oscillations in the dynamical evolution. Although the oscillation frequencies could have been foreseen quite easily, we also derive the associated damping rates and the relative weights, all of which could scarcely be guessed offhand. For the damping rates, we derive some known relations but add new results that fully determine the relative magnitude of the damping. In addition, an explicit evaluation of the power spectra leads to a neat discussion of the effect of the initial conditions on the relations among the peaks of the power spectra either for the same mode but at different frequencies or for different modes but at the same frequencies.

Finally, we show that there is a resonant situation in which the two internal frequencies Ω_R and Ω_L are commensurate. This requires a special analysis since otherwise there are divergencies. In the framework of the perturbation analysis carried out in this paper, there is no boundary layer connecting the resonant and the nonresonant situations. Such a boundary layer would require a different scaling to appear and be analyzed.

ACKNOWLEDGMENTS

This research was supported in part by the Fonds National de la Recherche Scientifique (Belgium) and the Interuniversity Attraction Pole program of the Belgian government.

APPENDIX A: DEFINITIONS OF L, M_1, AND M_2

The matrix L, and the vectors M_1 and M_2 appearing in Eqs. (8)–(10) are

$$L=\begin{pmatrix} m_1 & O' & \cdots & O' \\ R & m_2 & \cdots & O \\ \vdots & \vdots & \ddots & \vdots \\ R & O & \cdots & m_N \end{pmatrix},$$

where

$$m_1=\begin{pmatrix} 0 & -1 & 0 \\ NI & 0 & -I/2 \\ 0 & d-NQ & 0 \end{pmatrix}, \quad m_2=m_3=\cdots=m_N=\begin{pmatrix} 0 & -I/2 \\ d & 0 \end{pmatrix},$$

$$R=\begin{pmatrix} I & 0 & 0 \\ 0 & -Q & 0 \end{pmatrix}, \quad O'=\begin{pmatrix} 0 & 0 \\ 0 & 0 \\ 0 & 0 \end{pmatrix}, \quad O=\begin{pmatrix} 0 & 0 \\ 0 & 0 \end{pmatrix},$$

while

$$M_1=\mathrm{col}\left[\left(\frac{\partial^2}{\partial T_{-1}^2}-\frac{\partial}{\partial T_0}-1\right)\mathcal{D}_0,\frac{1}{2I}\sum_{q=1}^{N}\frac{\partial\mathcal{I}_{q0}^2}{\partial T_{-1}}-\frac{\partial\mathcal{I}_{T0}}{\partial T_0},NI\mathcal{D}_0-\left(\frac{\partial}{\partial T_0}+U\right)\mathcal{Q}_{T0},\frac{1}{2I}\frac{\partial}{\partial T_{-1}}\mathcal{I}_{20}^2-\frac{\partial\mathcal{I}_{20}}{\partial T_0},I\mathcal{D}_0\right.$$
$$\left.-\left(\frac{\partial}{\partial T_0}+U\right)\mathcal{Q}_{20},\frac{1}{2I}\frac{\partial}{\partial T_{-1}}\mathcal{I}_{30}^2-\frac{\partial\mathcal{I}_{30}}{\partial T_0},I\mathcal{D}_0-\left(\frac{\partial}{\partial T_0}+U\right)\mathcal{Q}_{30},\ldots,I\mathcal{D}_0-\left(\frac{\partial}{\partial T_0}+U\right)\mathcal{Q}_{30},I\mathcal{D}_0-\left(\frac{\partial}{\partial T_0}+U\right)\mathcal{Q}_{N0}\right] \tag{A1}$$

and

$$M_2=\begin{pmatrix}
\left(\frac{\partial^2}{\partial T_{-1}^2}-\frac{\partial}{\partial T_0}-1\right)\mathcal{D}_1+\left(\frac{2\partial}{\partial T_{-1}}\frac{\partial}{\partial T_0}-\frac{\partial^3}{\partial T_{-1}^3}+\frac{\partial}{\partial T_{-1}}-\frac{\partial}{\partial T_1}\right)\mathcal{D}_0 \\
\frac{1}{I}\frac{\partial}{\partial T_{-1}}\left[\sum_{q=1}^{N}\left(\mathcal{I}_{q0}\mathcal{I}_{q1}-\frac{\mathcal{I}_{q0}^3}{3I}\right)\right]+\frac{\partial}{\partial T_0}\left(\frac{1}{2I}\sum_{q=1}^{N}\mathcal{I}_{q0}^2-\mathcal{I}_{T1}\right)-\frac{\partial\mathcal{I}_{T0}}{\partial T_1} \\
\left(\mathcal{I}_{T0}+\mathcal{Q}_{T0}\frac{\partial}{\partial T_{-1}}\right)\mathcal{D}_0+NI\mathcal{D}_1-\left(\frac{\partial}{\partial T_0}+U\right)\mathcal{Q}_{T0}-\frac{\partial\mathcal{Q}_{T0}}{\partial T_1} \\
\frac{1}{I}\frac{\partial}{\partial T_{-1}}\left(\mathcal{I}_{20}\mathcal{I}_{21}-\frac{\mathcal{I}_{20}^3}{3I}\right)+\frac{\partial}{\partial T_0}\left(\frac{\mathcal{I}_{20}^2}{2I}-\mathcal{I}_{21}\right)-\frac{\partial\mathcal{I}_{20}}{\partial T_1} \\
\left(\mathcal{I}_{20}+\mathcal{Q}_{20}\frac{\partial}{\partial T_{-1}}\right)\mathcal{D}_0+I\mathcal{D}_1-\left(\frac{\partial}{\partial T_0}+U\right)\mathcal{Q}_{21}-\frac{\partial\mathcal{Q}_{20}}{\partial T_1} \\
\frac{1}{I}\frac{\partial}{\partial T_{-1}}\left(\mathcal{I}_{30}\mathcal{I}_{31}-\frac{\mathcal{I}_{30}^3}{3I}\right)+\frac{\partial}{\partial T_0}\left(\frac{\mathcal{I}_{30}^2}{2I}-\mathcal{I}_{31}\right)-\frac{\partial\mathcal{I}_{30}}{\partial T_1} \\
\left(\mathcal{I}_{30}+\mathcal{Q}_{30}\frac{\partial}{\partial T_{-1}}\right)\mathcal{D}_0+I\mathcal{D}_1-\left(\frac{\partial}{\partial T_0}+U\right)\mathcal{Q}_{31}-\frac{\partial\mathcal{Q}_{30}}{\partial T_1} \\
\vdots \\
\frac{1}{I}\frac{\partial}{\partial T_{-1}}\left(\mathcal{I}_{N0}\mathcal{I}_{N1}-\frac{\mathcal{I}_{N0}^3}{3I}\right)+\frac{\partial}{\partial T_0}\left(\frac{\mathcal{I}_{N0}^2}{2I}-\mathcal{I}_{N1}\right)-\frac{\partial\mathcal{I}_{N0}}{\partial T_1} \\
\left(\mathcal{I}_{N0}+\mathcal{Q}_{N0}\frac{\partial}{\partial T_{-1}}\right)\mathcal{D}_0+I\mathcal{D}_1-\left(\frac{\partial}{\partial T_0}+U\right)\mathcal{Q}_{N1}-\frac{\partial\mathcal{Q}_{N0}}{\partial T_1}
\end{pmatrix}. \tag{A2}$$

APPENDIX B: DEFINITIONS OF $M_1^{(j)}$

Here are the expressions for $M_1^{(j)}$ in Eq. (24):

$$M_1^{(0)}=\mathrm{col}\left(-\frac{A_0+\dot{A}_0}{2},0,N\mathcal{A}_0,0,\mathcal{A}_0,0,\mathcal{A}_0,\ldots,0,\mathcal{A}_0\right), \tag{B1}$$

$$M_1^{(L)}=\mathrm{col}\left(0,0,0,\frac{i\omega_L\dot{A}_{L,1}}{d},\mathcal{A}_{L,1},\frac{i\omega_L\dot{A}_{L,2}}{d},\mathcal{A}_{L,2},\ldots,\frac{i\omega_L\dot{A}_{L,N-1}}{d},\mathcal{A}_{L,N-1}\right), \tag{B2}$$

$$M_1^{(R)}=\mathrm{col}(a_R,-iNr\dot{A}_R,N\mathcal{A}_R,-ir\dot{A}_R,\mathcal{A}_R,-ir\dot{A}_R,\mathcal{A}_R,\ldots,-ir\dot{A}_R,\mathcal{A}_R), \tag{B3}$$

$$M_1^{(2L)}=ib\,\mathrm{col}(0,NA_L^2/I,0,A_{L,1}^2,0,A_{L,2}^2,0,\ldots,A_{L,N-1}^2,0), \tag{B4}$$

$$M_1^{(2R)}=igA_R^2\mathrm{col}(0,N/2I,0,1,0,1,0,\ldots,1,0), \tag{B5}$$

$$M_1^{(L-R)}=iA_R^*\mathrm{col}(0,0,0,h^{(-)}A_{L,1},0,h^{(-)}A_{L,2},0,\ldots,h^{(-)}A_{L,N-1},0), \tag{B6}$$

and

$$M_1^{(L+R)}=iA_R\mathrm{col}(0,0,0,h^{(+)}A_{L,1},0,h^{(+)}A_{L,2},0,\ldots,h^{(+)}A_{L,N-1},0). \tag{B7}$$

In the above expressions the following notations have been introduced:

$$\mathcal{A}_0=\left(\frac{I}{2}-U\right)A_0-\dot{A}_0,\mathcal{A}_{L,j}=-(UA_{L,j}+\dot{A}_{L,j}),\quad a_R=-\frac{N[(\omega_R^2+1)A_R+\dot{A}_R]}{NQ-d},$$

$$r=\frac{\omega_R}{NQ-d},\quad \mathcal{A}_R=\left(\frac{NI}{NQ-d}-U\right)A_R-\dot{A}_R,\quad A_L^2=\sum_{i=1}^{N-1}A_{L,i}^2+\sum_{j=i+1}^{N-1}\sum_{i=1}^{N-1}A_{L,i}A_{L,j},$$

$$b=\frac{2\omega_L^3}{d^2},\quad g=\frac{2\omega_R^3}{(NQ-d)^2},\quad h^{(\mp)}=\pm\frac{2\omega_L\omega_R(\omega_L\mp\omega_R)}{d(NQ-d)}.$$

The dot implies a derivative with respect to T_0.

APPENDIX C: NOTATIONS FOR $\mathcal{Z}_{1,par}$

This appendix defines the notations appearing in Eqs. (42)–(48):

$$\alpha=\frac{1}{\omega_R}[2w(N-2NQ+2d)-3NI+3U(NQ-d)],\quad \beta=2Nw+NI-U(NQ-d),$$

$$\vartheta=\frac{1}{\omega_R}[NI(NQ-8N-d)+U(8N-NQ-d)(NQ-d)-6Nw(NQ-d)],$$

$$\varphi_j=\mu\widetilde{B}_L^2-\nu\widetilde{B}_{L,j}^2,\quad \phi_j=x\widetilde{B}_L^2-y\widetilde{B}_{L,j}^2,\quad \widetilde{B}_L^2=\sum_{i=1}^{N-1}\widetilde{B}_{L,i}^2+\sum_{j=i+1}^{N-1}\sum_{i=1}^{N-1}\widetilde{B}_{L,i}\widetilde{B}_{L,j},$$

$$\mu=\frac{2}{3N\omega_L}(\omega_L^2-\omega_R^2),\quad \nu=\frac{2I}{3N\omega_L}(4\omega_L^2-\omega_R^2),\quad x=\frac{1}{3N\omega_L^2}[d(\omega_L^2-\omega_R^2)+3NQ\omega_L^2],$$

$$y=\frac{dI}{3N\omega_L^2}(4\omega_L^2-\omega_R^2),\quad \chi=\frac{2\omega_R}{4\omega_R^2-\omega_L^2}[\omega_L^2-\omega_R^2(1+6I)],$$

$$\eta=\frac{i}{4\omega_R^2-\omega_L^2}[NQ(4\omega_R^2-\omega_L^2)-d(\omega_R^2-\omega_L^2)-6dI\omega_R^2],\quad \omega^{(\pm)}=(\omega_L\pm\omega_R)/d.$$

APPENDIX D: DEFINITIONS OF $\widetilde{M}_2^{(j)}$

The matrices $\widetilde{M}_2^{(j)}$ in Eq. (52) are

$$\widetilde{M}_2^{(0)}=\mathrm{col}(\widetilde{b}_0,Na_1\widetilde{B}_0,N\widetilde{\mathcal{B}}_0,a_1\widetilde{B}_0,\widetilde{\mathcal{B}}_0,a_1\widetilde{B}_0,\widetilde{\mathcal{B}}_0,\ldots,a_1\widetilde{B}_0,\widetilde{\mathcal{B}}_0),\tag{D1}$$

$$\widetilde{M}_2^{(L)}=\mathrm{col}(0,0,0,\widetilde{\mathcal{B}}_{L,1},\widetilde{b}_{L,1},\widetilde{\mathcal{B}}_{L,2},\widetilde{b}_{L,2},\ldots,\widetilde{\mathcal{B}}_{L,N-1},\widetilde{b}_{L,N-1}),\tag{D2}$$

and

$$\widetilde{M}_2^{(R)}=\mathrm{col}(N\beta_R,N\widetilde{\mathcal{B}}_R,N\widetilde{b}_R,\widetilde{\mathcal{B}}_R,\widetilde{b}_R,\widetilde{\mathcal{B}}_R,\widetilde{b}_R,\ldots,\widetilde{\mathcal{B}}_R,\widetilde{b}_R).\tag{D3}$$

In Eqs. (D1)–(D3)

$$\widetilde{b}_0=[(\Gamma_0-1)\widetilde{B}_0-\widetilde{B}_0']/2,\quad \widetilde{\mathcal{B}}_0=\Gamma_0\widetilde{B}_0-\widetilde{B}_0',\quad \widetilde{\mathcal{B}}_{L,j}=(ia_2+a_3)\Gamma_L\widetilde{B}_{L,j}-ia_2\widetilde{B}_{L,j}',$$

$$\widetilde{b}_{L,j}=(1-ia_4)\Gamma_L\widetilde{B}_{L,j}-\widetilde{B}_{L,j}',\quad \beta_R=[(a_5+ia_6)(\Gamma_R-w)-ia_5w\omega_R]\widetilde{B}_R-a_5\widetilde{B}_R',$$

$$\widetilde{\mathcal{B}}_R=(a_7+ia_8)\Gamma_R\widetilde{B}_R-ia_8\widetilde{B}_R',\quad \widetilde{b}_R=\Gamma_R\widetilde{B}_R-\widetilde{B}_R',\quad a_1=\frac{(2N-1)\Gamma_0I^2}{4\omega_R^2},\quad a_2=-\frac{\omega_R}{d},$$

$$a_3=\frac{U}{4d},\quad a_4=-\frac{U}{4\omega_R},\quad a_5=-\frac{I}{2(d-1)},\quad a_6=\frac{\alpha I}{4\omega_R^2},\quad a_7=\frac{\beta a_6}{\alpha},\quad a_8=\omega_Ra_5.$$

The prime denotes a derivative with respect to T_1.

APPENDIX E: DEFINITIONS OF THE MATRICES $M_1^{(0,1,2,3,4)}$

The matrices $M_1^{(0,1,2,3,4)}$ appearing in Eq. (78) are

$$M_1^{(0)}=\mathrm{col}\left(-\frac{A_0+\dot{A}_0}{2},0,-\frac{7A_0}{2}-2\dot{A}_0,0,-\frac{7A_0}{4}-\dot{A}_0\right),$$

$$M_1^{(1)}=\mathrm{col}\left(0,0,0,\frac{i}{4}\sqrt{\frac{7}{2}}(\dot{A}_L-2A_L^*A_R),-2A_L-\dot{A}_L\right),$$

$$M_1^{(2)}=\mathrm{col}\left(\frac{15A_R+7\dot{A}_R}{2},\frac{i}{2}\sqrt{\frac{7}{2}}(A_L^2+4\dot{A}_R),-\frac{15A_R+4\dot{A}_R}{2},\frac{i}{8}\sqrt{\frac{7}{2}}(A_L^2+8\dot{A}_R),-\frac{15A_R+4\dot{A}_R}{4}\right),$$

$$M_1^{(3)}=\frac{3i}{2}\sqrt{\frac{7}{2}}A_LA_R\mathrm{col}(0,0,0,1,0),$$

and

$$M_1^{(4)}=2i\sqrt{14}A_R^2\mathrm{col}(0,2,0,1,0).$$

[1] C. L. Tang, H. Statz, and G. deMars, J. Appl. Phys. **34**, 2289 (1963).
[2] P. Mandel, *Theoretical Problems in Cavity Nonlinear Optics* (Cambridge University Press, Cambridge, 1997).
[3] K. Wiesenfeld, C. Bracikowski, G. James, and R. Roy, Phys. Rev. Lett. **65**, 1749 (1990).
[4] T. Erneux and P. Mandel, Phys. Rev. A **52**, 4137 (1995).
[5] K. Otsuka, P. Mandel, S. Bielawski, D. Derozier, and P. Glorieux, Phys. Rev. A **46**, 1692 (1992).
[6] S. Bielawski, D. Derozier, and P. Glorieux, Phys. Rev. A **46**, 2811 (1992).
[7] P. Mandel, M. Georgiou, K. Otsuka, and D. Pieroux, Opt. Commun. **100**, 341 (1993).
[8] K. Otsuka, Phys. Rev. Lett. **67**, 1090 (1991).
[9] N. B. Abraham, L. L. Everett, C. Iwata, and M. B. Janicki, Proc. SPIE **2095**, 16 (1994).
[10] B. A. Nguyen and P. Mandel, Opt. Commun. **112**, 235 (1994).
[11] D. Pieroux, T. Erneux, and P. Mandel, Phys. Rev. A **54**, 3409 (1996).
[12] K. Otsuka, M. Georgiou, and P. Mandel, Jpn. J. Appl. Phys., Part 2 **31**, L1250 (1992).
[13] P. Le Boudec, C. Jaouen, P. L. François, J.-F. Bayon, F. Sanchez, P. Besnard, and G. Stephan, Opt. Lett. **18**, 1890 (1993).
[14] K. Otsuka, P. Mandel, M. Georgiou, and C. Etrich, Jpn. J. Appl. Phys., Part 2 **32**, L318 (1993).
[15] E.A. Victorov, D. R. Klemer, and M. A. Karim, Opt. Commun. **113**, 441 (1995).
[16] J. Wang, P. Mandel, and T. Erneux, Quantum Semiclassic. Opt. **7**, 169 (1995).
[17] K. Y. Tsang, R. E. Mirollo, S. H. Strogatz, and K. Wiesenfeld, Physica D **48**, 102 (1991).
[18] D. G. Aronson, M. Golubitsky, and J. Mallet-Paret, Nonlinearity **4**, 903 (1991).
[19] M. Silber, L. Fabiny, and K. Wiesenfeld, J. Opt. Soc. Am. B **10**, 1121 (1993).
[20] W.-J. Rappel, Phys. Rev. E **49**, 2750 (1994).
[21] S. Watanabe and S. H. Strogatz, Phys. Rev. Lett. **70**, 2391 (1993).
[22] G. B. Ermentrout, Physica D **41**, 219 (1990).
[23] P. C. Matthews and S. H. Strogatz, Phys. Rev. Lett. **65**, 1701 (1990).
[24] P. Mandel, K. Otsuka, J. Y. Wang, and D. Pieroux, Phys. Rev. Lett. **76**, 2694 (1996).
[25] P. Mandel and J.-Y. Wang, Phys. Rev. Lett. **75**, 1923 (1995); **76**, 1403(E) (1996).
[26] B. A. Nguyen and P. Mandel, Phys. Rev. A **54**, 1638 (1996).
[27] P. Mandel, B. A. Nguyen, and K. Otsuka, Quantum Semiclassic. Opt. **9**, 365 (1997).
[28] L. Stamatescu and M. W. Hamilton, Phys. Rev. E **55**, R2115 (1997).
[29] D. Pieroux and P. Mandel, Opt. Commun. **107**, 245 (1994).
[30] P. A. Khandokhin, P. Mandel, I. V. Koryukin, B. A. Nguyen, and Ya. I. Khanin, Phys. Lett. A **235**, 248 (1997).
[31] B. A. Nguyen and P. Mandel, Opt. Commun. **138**, 81 (1997).
[32] P. A. Khandokhin, Ya. I. Khanin, J.-C. Celet, D. Dangoisse, and P. Glorieux, Opt. Commun. **123**, 372 (1996).
[33] Ya. I. Khanin, *Principles of Laser Dynamics* (Elsevier, Amsterdam, 1995).
[34] A. V. Ghiner, K. P. Komarov, and K. G. Folin, Opt. Commun. **19**, 350 (1975).
[35] P. A. Khandokhin, P. Mandel, I. V. Koryukin, B. A. Nguyen, and Ya. I. Khanin, Izv. Vyssh. Uchebn. Zaved. Radiofiz. **40**, 161 (1997).